Applied Nanoscience (2022) 12:2829–2839
https://doi.org/10.1007/s13204-022-02595-3

ORIGINAL ARTICLE

Modification of polyester filters with synthesized copper nanoparticles for use as biocide in a real environment

K. Machry[1] · M. L. Aguiar[1] · C. W. O. de Souza[2] · A. Bernardo[1]

Received: 15 February 2022 / Accepted: 31 July 2022 / Published online: 18 August 2022

Abstract

Antimicrobial air filtration techniques have recently been widely studied to enhance indoor air quality and mitigate hazardous airborne microorganisms. Here, CuNPs were incorporated into a commercial polyester fiber surface and Scanning Mobility Particle Sizer was used to measure the adherence between fibers and nanoparticles. An acid pretreatment previous CuNP incorporation was effective against the particle release and enhanced the adhesion between particle and fiber. CuNP was a mixture of Cu^0 and Cu_2O with a diameter size of 90 nm (SEM micrographs). The permeability of the filter was low, in order of 10^{-9} m^2. The activity against pathogens was tested in loco in a real environment using a filtration prototype apparatus. It was observed that the presence of CuNP mitigated the fungi and bacteria growth not only on the surface but also reduced microbe concentrations after passing through the filter. These results show that CuNP can be used as an inhibitor of various microorganisms, making them a good alternative for indoor environments to control indoor air quality.

Keywords Acid pretreatment · Nanoparticle release · CuNP · Adhesion · Air quality · Indoor environments

Introduction

Many diseases can be airborne transmitted, such as the common cold, influenza, Ebola, tuberculosis, chickenpox, and measles. Aerosol transmissions by droplets are the main risk for airborne pathogens and diseases, such as observed in the COVID-19 pandemic, where mask dressing was recommended to avoid the virus transmission. Studies also have shown that pathogens, such as viruses, can be transmitted by plastic, stainless steel, and copper surfaces (Warnes et al. 2015). Materials such as masks, purifiers, or even filters for air filtration with biocide activity can play an important role in airborne filtration. It can improve the air quality and human health, especially in indoor environments, in which the probability of human transmission of pathogens microorganisms, and diseases is higher than in outdoor environments (Ahlawat et al. 2020; Yao et al. 2020).

✉ A. Bernardo
abernardo@ufscar.br

[1] Department of Chemical Engineering, Federal University of São Carlos, São Carlos, São Paulo, Brazil

[2] Department of Morphology and Pathology, Federal University of São Carlos, São Carlos, São Paulo, Brazil

Materials with antibacterial activity can be also used in medical tools for healthcare workers (Nakamura et al. 2019), wound dressing, masks (Tremiliosi et al. 2020), and even air filters (Hwang et al. 2015). In public environments, such as air-conditioning systems (taxis, buses, hospitals, and hotels), the implementation of a biocide filter can improve the safety of handling and discarding of those products. By inactivating pathogens on the surface of the filter, it can improve the air quality of indoor environments (Garciá De Abajo et al. 2020). The air filter is the first barrier between the external and internal environment and is a favorable place for chemical reactions and the growth of microorganisms. Considering this, it is possible to combine metal nanoparticles with masks or filters (Hashmi et al. 2019) and provide safety by reducing the growth of microorganisms on these surfaces.

Silver is a precious metal widely explored due to its antimicrobial effect (AshaRani et al. 2009; Bortolassi et al. 2019), but its high cost and the technology to impregnate in commercial filters can increase the cost of the final product by silver addition. Copper is a well-known metal with antimicrobial and antiviral properties (Patil et al. 2022). The global market of precious metals indicates that the cost of copper is considerably lower than silver (Balcilar and Ozdemir 2019). Copper also is known due to its electronic conductivity, fungicidal effect, bactericidal and antiviral

effect (Bogdanovic et al. 2014; Warnes et al. 2015). Applying copper in masks, in air conditioning, or portable air filters may be more cost-effective than using silver and the efficiency against pathogens can be equal to or even higher than using silver (Tang et al. 2018).

The application of nanoparticles in air filters can be promising; however, nanoparticle release in the environment may be a challenge. Nanoparticles in conventional methods are deposited externally and are not firmly fixed, leading to a contamination of the environment. A wet chemical treatment in polyester fiber filters does not require special equipment, it is cost-effective and seems to be a good option for increasing the adhesion between fiber and nanoparticle (Baley et al. 2006; Cammarano et al. 2013). The antimicrobial activity of copper nanoparticles can improve the safety of materials, such as medical tools for healthcare workers (Nakamura et al. 2019), masks (Tremiliosi et al. 2020), and even air filters (Hwang et al. 2015).

This paper is mainly focused on the utilization of CuNP in air conditioning filters for antimicrobial applications. The antimicrobial analysis was developed in loco, in a real environment, using a prototype apparatus for air filtration. Thanks to the CuNP, the modified filter can be used to mitigate hazardous airborne microorganisms and improve the air quality of indoor rooms. This study provides new insights into the development of smart air filters, in which CuNP can be used in portable air filters, purifiers, and masks.

Materials and methods

Synthesis and characterization of nanoparticles

CuNPs were synthesized by a redox reaction (Liu et al. 2012). In brief, a 0.2 mol/L solution of $CuSO_4.5H_2O$ was prepared, and added 15 mmol/L of PVP as the capping agent in 100 mL. In another Erlenmeyer, 40 mL of a 1.0 mol/L solution of ascorbic acid was prepared. The pH of the solutions was adjusted to 7 using NaOH and ultrasonicated. The reaction was initiated by mixing both solutions under controlled temperature (70 °C) and agitation (70 rpm) for 4 h. As the reaction occurred, the color of the suspension reached to ocher, indicating the presence of CuNP. The suspension was maintained at room temperature for 12 h to precipitate. Particles were centrifuged (DAIKI, 80-2B) at 4000 rpm (2325 g) for 10 min and washed with distilled water to remove the supernatant. The nanoparticles were maintained in a solution with distilled water [0.1% (w/w)] for approximately 2 months.

CuNP was characterized by X-ray diffraction (Bucker XRD D8 Advance) with Cu Kα radiation (1.5418 Å) in the scanning range of 2θ between 20° and 70°. The crystallite size from the XRD diffraction pattern was used in the Scherrer equation, shown in Eq. 1:

$$\mathrm{FMHM}(2\theta) = \frac{b \cdot \lambda}{D \cdot \cos\theta} \quad (1)$$

in which FMHM (2θ) is the line broadening at half the maximum intensity, in radians; b is the Scherrer constant, related to the shape, which normally ranges between 0.89 and 0.94, and for nanoparticles, its value is 0.9 (Holder and Schaak 2019). λ is the X-ray wavelength ($\lambda = 0.154$ nm); D is the averaged dimension of crystallites in nanometers (in nm); θ is the Bragg angle, that corresponds to the position of the diffraction peak maximum, in rad.

The CuNP suspension was characterized in DSL—Sizer (NANO ZS90)—to measure the hydrodynamic size of the sample. A 1:500 dilution of the CuNP suspension (0.1% w/w) was used to measure by dynamic light scattering.

Polyester filter and coating with CuNP

The polyester filter medium was provided by FILTRACOM company from Valinhos, Brazil. The filter is commercially sold for air conditioning systems. The filter has a thickness of 5.5 ± 1.5 mm, a grammage of $180 \pm 10\%$ g/m^2, and efficiency in the range of 80 and 90% to particles above 0.4 µm.

The CuNP suspension (10 g of 0.1% w/w suspension) was previously ultrasonicated and used to impregnate a 144 cm^2 polyester filter. The coating was performed by spraying uniformly at the face filter at 10 cm the CuNP suspension, using a commercial bottle spray. The excess water was removed in an oven for 24 h at 50 °C and the impregnated filters were stored in airtight bags before use. The nanoparticle concentration (0.08 mg_{CuNP}/cm^2) was measured by gravimetry.

To enhance the adhesion between fiber and nanoparticle, a chemical pretreatment was performed before the CuNP impregnation in a 0.01 M solution of HCl (37%) and the sample of the polyester filter was submerged for 5 min. Filter without modification are identified as untreated (control group). Filter just treated with CuNP are identified as CuNP treated. The filter acidly treated previous to the CuNP coating is identified as Acid and CuNP treated.

Filter characterization

Scanning Electron Microscopy (SEM) (FEI Magellan 400) was used to evaluate the morphology of the filter and the nanoparticles impregnated in the filter medium. The energy-dispersive X-ray (EDS) system was used for the chemical mapping of the sample.

The permeability of filters was measured by monitoring the pressure loss using a digital manometer (TSI 955—P). The airflow was increased gradually, the loss of pressure was

verified in a rotameter and the data were collected. The range flow was chosen based on previous work from the research group with values between 0 and 37 L/min to ensure a high range of air velocity (Rosa et al. 2017). The angular coefficient of the plot ($\Delta P/\Delta x$ versus v) was used to measure the permeability, based on Darcy's Law (Eq. 2). The thickness of the filter medium was measured using a digital caliper, with a value of 4.15 ± 0.05 mm and the air viscosity was $1.84 \cdot 10^{-5}$ Pa.s.

$$\frac{\Delta P}{\Delta x} \cdot \frac{1}{v} = \frac{\mu}{k} \tag{2}$$

In which ΔP (Pa) is the loss of pressure across the filter medium; Δx (m) is the thickness of the filter; v (m/s) is the air velocity of the airflow; μ (Pa.s) is the air viscosity and k (m^2) the Darcy's constant.

CuNP release

The CuNP adhesion in the fiber filter was evaluated by measuring the nanoparticle release in Scanning Mobility Particle Sizer (SMPS)®. The filter was positioned in the support for fibers of the equipment with the face impregnated with CuNP contrary to the airflow. As the airspeed was gradually increased, the count of particles upstream and downstream of the filter was measured in triplicate using a particle counter. The diameter and the count of nanoparticles for each airflow were measured in SMPS, coupled with a Condensation Particle Counter (TSI 3080) and an Electrostatic Classifier (TSI 3776). For each filter (untreated, CuNP treated, acid and CuNP treated). The data are shown in $dW/dlogD_p$, which corresponds to the concentration of particles in $\#/cm^3$.

Microbial analysis in a real environment

To study the antimicrobial effect of the filter impregnated with CuNP, a prototype apparatus (Catranis et al. 2006) was used to simulate airborne filtration in a real environment (Fig. 1). This analysis consists of a comparison between the untreated filter and the acid and CuNP-treated filter, simultaneously. In the prototype, we simulate filtration, such as in an air conditioning system, using a pump to make sure the air is passing through the filter at 600 L/h. The two filter apparatuses were set up side by side. The HEPA filters help us to make sure that all the microbes, which eventually pass through the filters, are retained below. Each filtration system's pump is turned on simultaneously and the airflow is adjusted at 600 L/h. At the end of each experiment, we have the comparison between the untreated (and HEPA untreated) and the filter acid and CuNP treated (and the HEPA of the same filter). To compare the results, we observed the retained microorganism colonies in the untreated and may compare with the retained colonies of the acid and CuNP-treated filter. This comparison can lead us to conclude if the presence of nanoparticles in the filter can avoid the proliferation of microorganisms on the surface of the filter.

The airflow was set at 600 L/h, which corresponds to a velocity of 2 m/s, to simulate the breathing of a person at rest

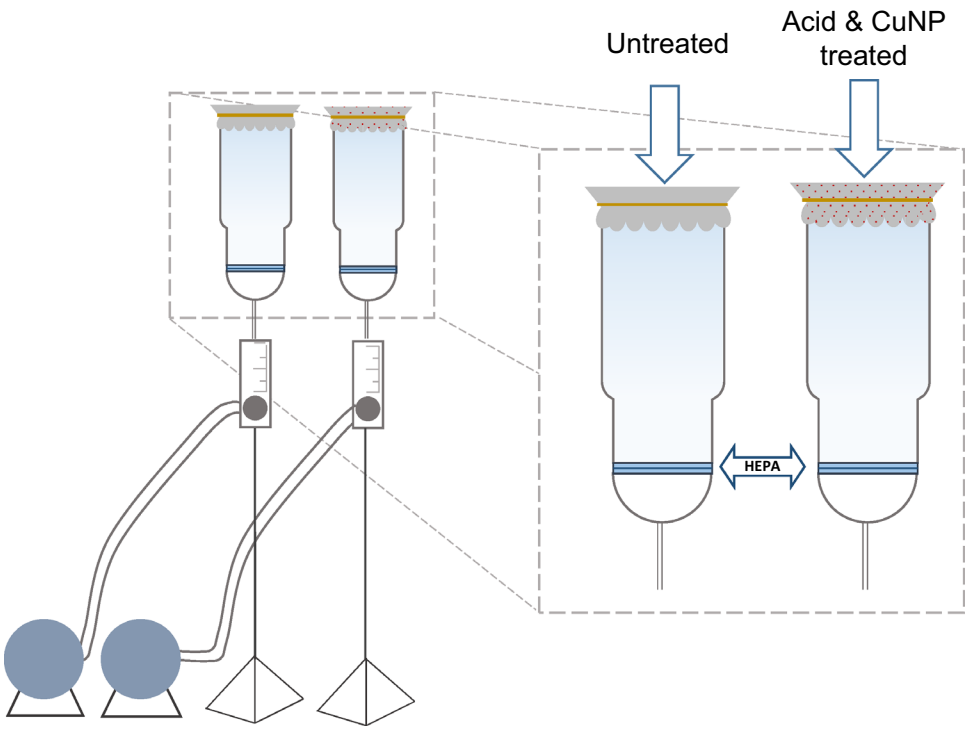

Fig. 1 Schematic illustration of the real environment test with details of filtration component

or even the velocity of an air conditioning system (between 1 and 5 m/s) (Rosa et al. 2017). The collection in loco was in a toilet in Department of Chemical Engineering for 1 h (I), in a hall in the Department of Chemical Engineeringhall for 6 h (II) and in an external environment for 24 h (III). The removal of the filter from the support was performed in a laminar flow hood using forceps flamed. The filters were removed and added to an Erlenmeyer with phosphate-buffered saline (PBS) to release fiber-associated microbes from the filter material into the PBS. To the filters (untreated and acid and CuNP treated) was added a sufficient PBS volume to recover the filter (50 mL), and HEPA filter (10 mL). The solution was maintained for 30 min under agitation (60 rpm) and after submitted for 10 min into an ultrasonicated bath to release all the microbial content present in the fiber to the PBS solution.

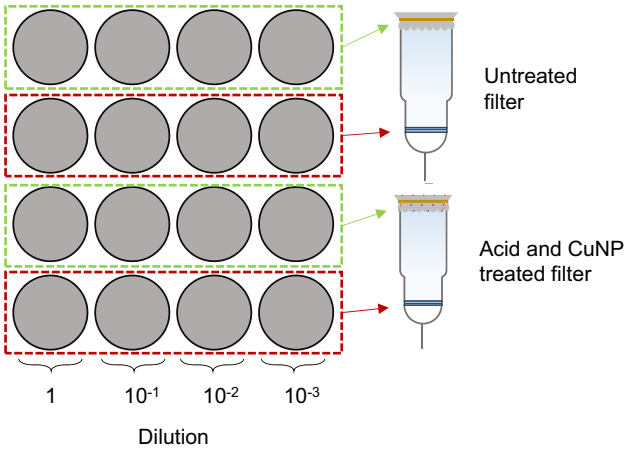

Fig. 2 Schematic diagram of the samples. Vertically, the plaques of serial dilution. Horizontally the filter and HEPA of untreated sample (control), the acid and CuNP treated, and the HEPA, respectively

Antimicrobial quantification

The Tryptone Soya Agar (TSA—Oxoid CM0131) and Sabouraud Dextrose Agar (SAB—Oxoid CM0041) solutions were prepared according to the manufacturer's specifications. The filtered suspension was serially diluted. 100 µL was distributed across the agar plate using the spread plate technique. Plates were incubated for about 6 days, at 37 °C for TSA and 27 °C for SAB medium.

The analysis in a real environment aimed to determine if the presence of CuNP in the fiber filter can mitigate microorganisms in the fiber filter. The prototype used in this experiment follows the basic principle of filtration, in which the external air is forced to pass through the filter due to the suction of the air from the pump. The material retained in the filter depends on the efficiency of the filter (80–90% for particles above 0.4 µm), and all the material which passes through the filter is retained at HEPA (99.97% for particles above 0.3 µm). The schematic diagram of the samples is shown in Fig. 2.

Results and discussion

Synthesis and characterization of the CuNP

The color of the suspension was blue and after reaction time (4 h), it turned to ocher, indicating the redox reaction of Cu^{2+} ions in Cu^0 and the formation of the nanoparticles. The XRD pattern was analyzed in the software HighScore Plus and the result is shown in Fig. 3, in which the characteristics peaks of the suspension were a mixture of copper oxide (Cu_2O) and metallic copper (Cu).

As shown in Fig. 3, the suspension is composed of copper oxide and metallic copper. Liu et al. (2012) found the same compounds and suggested that Cu_2O corresponds to the intermediate product, produced by the transformation of Cu^{2+} ions from the precursor salt in $Cu(OH)_2$ after the adjustment of the pH. Then, the $Cu(OH)_2$ was reduced to Cu_2O by the redox reaction with ascorbic acid, to finally be reduced to Cu^0 particles (Liu et al. 2012). The chemical reaction follows the reduction process:

$$Cu(OH)_2+C_6H_8O_6 \rightarrow Cu_2O+C_6H_6O_6+H_2O$$

$$Cu_2O+C_6H_8O_6 \rightarrow Cu+C_6H_6O_6+H_2O$$

Diffractogram peaks at 29°, 36°, 42°, and 61° indicate the presence of Cu_2O, which corresponds to crystallographic planes at [110], [111], [200], and [220] for copper oxide, respectively. Peaks at 43° and 50° correspond to metallic copper (Cu^0) at crystallographic peaks at [111] and [200], respectively. To simplify, Cu_2O and Cu^0 are referred as CuNP in all this work and when relevant, the species will be mentioned as Cu_2O and Cu^0. The crystallite size of the nanoparticles determined by Eq. 1 was 37.88 ± 14.32 nm using the diffractogram pattern peaks shown in Fig. 3. In the monovalent copper form, cuprous oxide (Cu_2O) seems to be strongly effective against influenza viruses, more even than the divalent form of cupric oxide (CuO) (Hashimoto et al. 2017), indicating that even in low quantities, the cuprous oxide can be applied as an agent for virus inactivation. The metallic form of the nanoparticle (Cu^0) is also demonstrated to be effective against pathogen microorganisms, such as *E. coli*, *S. aureus*, and *C. albicans*, reducing 99.9% of *E. coli* bacteria in 2 h in contact (Bogdanovic et al. 2014). The interaction between nanoparticles and microorganisms can be very complex due to the composition, size, and shape of the nanoparticle (Albanese et al. 2012).

Fiber filters were coated with synthesized nanoparticles. Figure 4 shows SEM micrographs of the fiber surface structure and CuNP particles, in which CuNP are shown with a yellow arrow.

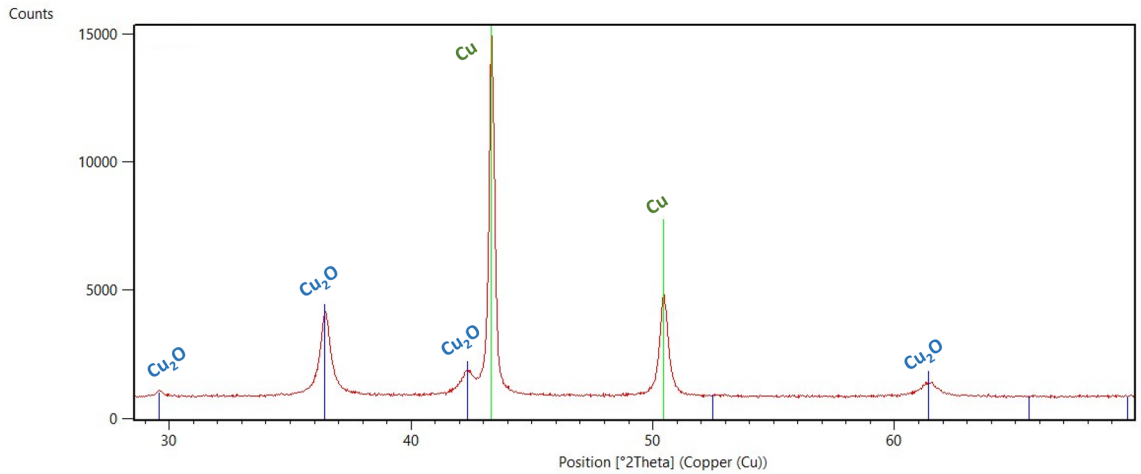

Fig. 3 XRD patterns of the obtained nanoparticles. The characteristic peaks of copper oxide (Cu_2O) are represented in blue and metallic copper (Cu^0) is represented in green

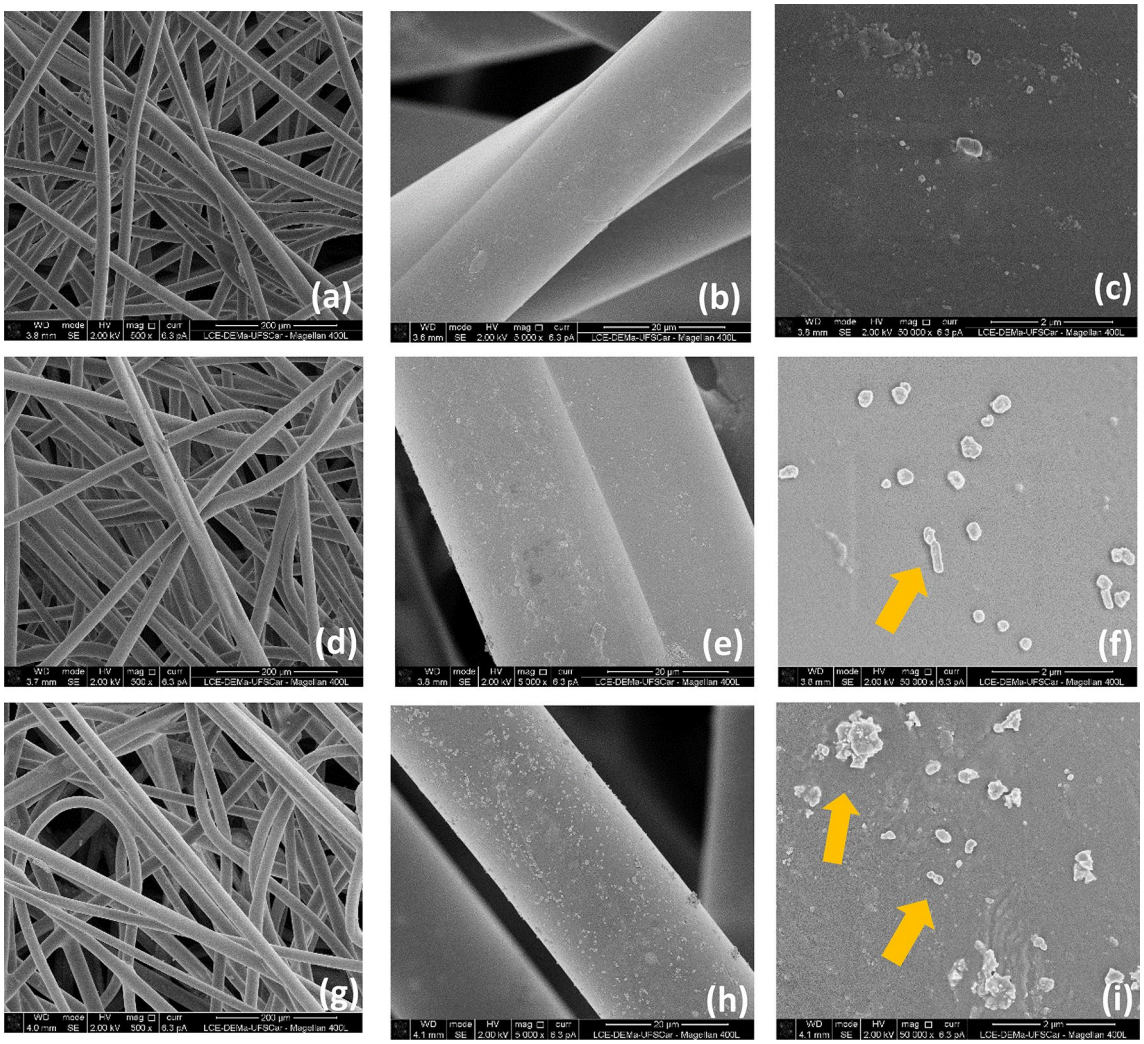

Fig. 4 SEM micrographs of the fiber filters of the untreated filter (**a**–**c**), CuNP-treated (**d**–**f**) and acid and CuNP-treated filter (**g**–**i**) in different magnitudes scales

Figure 4a–c shows the visual aspect in SEM micrographs of the polyester fiber fibers of the commercial filter. The arrow in yellow (Fig. 4c) indicates the presence of some dirt in the fiber, which is visually similar to a nanoparticle; however, EDS analysis was not capable to detect the presence of the element copper (0.14 ± 0.80% of Cu in EDS analysis). The dirt in the fiber is very common in commercial filters due to the handling and stock of the material. Filter CuNP coated micrographs are shown in Fig. 4d–f and filter Acid and CuNP are treated in Fig. 4g–i, respectively. To measure the particle size and fiber diameter, SEM micrographs were used in ImageJ software. The mean diameter of the fibers was obtained from 20 measurements in each SEM micrograph, and the average size was 25.17 ± 3.79 µm. Synthesized nanoparticles showed an average diameter of 90.32 ± 46.42 nm. The difference between the average diameter in SEM and XRD is mainly due to the different techniques of measurements. SEM can measure the cluster and the aggregation by cohesion force between particles, while XRD analysis measures the crystallite size of the nanoparticle. The difference between values corroborates that the CuNP mixture is a polycrystalline sample (Holder and Schaak 2019). Further discussions about the CuNP characterization can be found in our previous publication (Machry et al. 2021).

To measure the hydrodynamic size of the CuNP suspension, the initial suspension (0.1% w/w) was diluted at the ratio of 1:500 in distilled water and measured in dynamic light scattering, and the size distribution is shown in Fig. 5.

Figure 5 shows the hydrodynamic size distribution of the synthesized particles, one peak at 125 nm and another one at 500 nm. The first peak of less intensity occurred at approximately 125 nm and the second peak occurred at ~ 500 nm. The range size was from 100 to 750 nm. The hydrodynamic size distribution of the colloidal particles is polydisperse, with a PdI value of 0.59 and the hydrodynamic mean size was 557.2 ± 98.3 nm. The suspension was considered stable, once the zeta potential was − 31.4 mV, and stable suspensions have absolute zeta potential of 30 mV or higher (Ramírez-García et al. 2018). Stable suspensions have less tendency to agglomerate; however, in the present study, it was observed that nanoparticles formed some agglomerates, as shown in Fig. 4i.

The agglomeration occurs due to the small size of nanoparticles and high surface energy. Comparing the CuNP size by XRD, SEM, and DLS techniques, the difference between values indicates that the synthesized CuNP has high attraction forces, resulting in agglomerates, which can be seen in Fig. 4i and confirmed by the DLS analysis as the polydisperse sample.

Permeability of the polyester commercial filter medium modified with CuNP

The permeability is an important transport property, which measures the ability of the flow of fluids to percolate fibrous materials (Miguel 2003; Zhu et al. 2017). To measure the permeability is important to use filters of similar grammage to mitigate the effect of unequal fiber distribution. Filters with similar weight (area of 144 cm^2) were selected and the loss of pressure was measured for the untreated, CuNP treated and acid and CuNP treated. Table 1 shows the grammage, in g/m^2 and Darcy's constant permeability (k) calculated by Eq. 2. Results are expressed in average and standard deviation, in triplicate.

Table 1 shows the grammage and the permeability of the polyester filter untreated, CuNP treated and Acid and CuNP treated. Permeability evaluates the physical parameters of the fiber filter, such as the density of fibers, weight, and thickness (Anban and Vel). The permeability

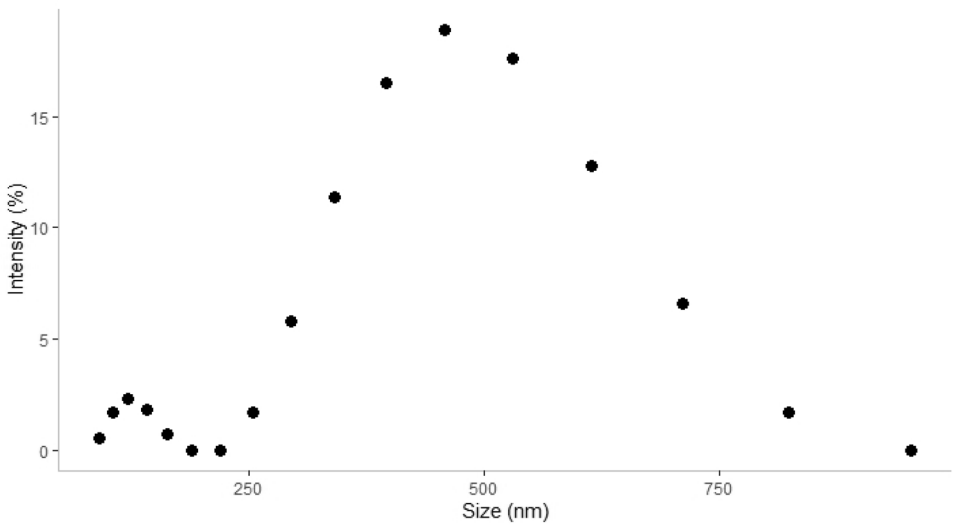

Fig. 5 Size distribution in DLS analysis of the synthesized CuNP, in a dilution of 1:500 of the initial CuNP suspension (0.1% w/w) in water

Table 1 Grammage, in g/m^2, and permeability (k), in m^2, of untreated, CuNP treated and acid and CuNP-treated filters

Filter medium	Grammage[a] (g/m^2)	k[a] (m^2)
Untreated	183.52 ± 3.79	$1.82 \cdot 10^{-9} \pm 3.54 \cdot 10^{-10}$
CuNP treated	181.79 ± 17.32	$1.84 \cdot 10^{-9} \pm 8.09 \cdot 10^{-10}$
Acid and CuNP treated	181.94 ± 2.19	$1.82 \cdot 10^{-9} \pm 4.33 \cdot 10^{-10}$

[a]Average and standard error filters in triplicate

was in the order of 10^{-9} m^2, which means the pressure drop (ΔP) across the filter at 5 cm/s was 20.36 Pa, 19.93 Pa, 20.29 Pa for untreated, CuNP treated, and acid and CuNP treated, respectively. The permeability of these polyester filters was of the same magnitude as HEPA filters (10^{-9} m^2) (Bortolassi et al. 2017); however, the pressure drop was considerably lower than HEPA filters, where Bortolassi et al. (2017) found the loss of pressure at 5 cm/s in range of 269 and 418 Pa.

When comparing the untreated filter to the two CuNP-impregnated filter types, no difference in filter permeability was detectable. The use of filters with similar grammage is important for the permeability measurement, because a higher concentration of fibers in the filter can increase air passage resistance, increasing *k*. Rosa et al. (2017) studied the impregnation of silver nanoparticles in cotton textiles, and the results are in agreement with our work, showing that the presence of nanoparticles in fibers does not influence air permeability.

CuNP release from the filter

Given the fact that nanoparticles released in the environment can cause serious risks for ecosystem and for human health (Hu and Zhou 2013), the adhesion between fiber and nanoparticle is important topic of study to mitigate risks. The nanoparticle's attachment to the fiber filter was measured in Scanning Mobility Particle Sizer™ (SMPS™). Particle concentration was counted upstream and downstream of the filter when submitted to a crescent airflow. The concentration of particles released at each airflow is indicated in Fig. 6 and the global average of nanoparticles released, considering the particle distribution, of the CuNP treated and acid and CuNP treated, respectively, are indicated in Table 2a, b.

Results suggested that acid pretreatment may play a role in the nanoparticle release by increasing the adhesion between fiber and particle. In Fig. 6 was possible to observe the acid treatment influenced positively in the adhesion force between fibers and CuNP, because have more points of dW/dlogDp to the surface without acid pretreatment. Figure 6 also shows the higher concentration of CuNP is released up to 100 nm, indicating that the dynamic diameter of those nanoparticles is in this range of size. The particle range between 0 and 200 nm in Fig. 6 corroborates with DLS analysis, which indicates that the CuNP sizes are polydisperse in the suspension, and a wide range of particle sizes can be found in suspension.

Based on the results, the acid treatment can modify the charge of the fiber, and the nanoparticles can adhere more strongly than when not applied to the acid treatment. As shown in Fig. 4i, agglomerates of CuNP were formed on the surface fibers. These agglomerates were formed by the high cohesion force between nanoparticles and electrostatic charge on the surface, leading to agglomeration. Jeyaraj et al. (2015) suggest that the acid chemical treatment cleans the fiber before the impregnation of natural dyes. For a concentrated alkaline medium, Nguyen et al. (2019) suggested that the chemical pretreatment in PET filters leads to a mass loss, degrading the fiber due to the concentrated medium.

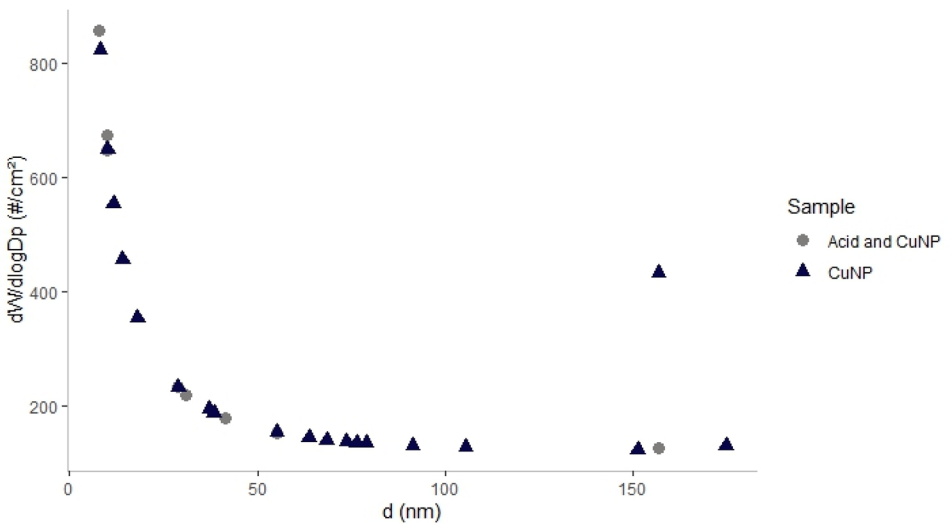

Fig. 6 Release of CuNPs from the CuNP-treated filter and the acid and CuNP-treated filter

Table 2 Global average numeric concentration of released particles (in #/cm^3) in the size of 3–300 nm detected for filters CuNP treated, and acid and CuNP treated, upstream and downstream of the filters for (a) CuNP treated and (b) acid and CuNP treated

(a) CuNP treated		
Flow (L/min)	Upstream the filters[a]	Downstream the filters[a]
4	0.66 ± 1.15	12.60 ± 3.12
7.5	1.30 ± 1.13	2.43 ± 2.20
14	0.00 ± 0.00	3.12 ± 3.65
15	0.68 ± 1.18	0.74 ± 1.28
18	0.00 ± 0.00	2.51 ± 4.34
18.4	5.60 ± 6.50	0.00 ± 0.00
21	0.00 ± 0.00	4.29 ± 7.42
(b) Acid and CuNP treated		
Flow (L/min)	Upstream the filters[a]	Downstream the filters[a]
1.5	1.47 ± 1.30	1.79 ± 1.72
2.5	1.97 ± 0.00	6.41 ± 0.00
6	0.00 ± 0.00	3.37 ± 5.85
6	7.05 ± 7.28	4.30 ± 5.52
9	0.00 ± 0.00	2.99 ± 5.19
14	0.00 ± 0.00	6.86 ± 11.87
14.5	3.02 ± 2.87	0.00 ± 0.00

[a]Measurements were performed with two CuNP-treated filters and results are expressed in mean ± standard deviation

In the present work, we did not verify a degradation of the fiber, probably due to the low concentration of our acid pretreatment and low time of contact (5 min). The mild condition of the acid pretreatment performed in the present work has positively increased the adhesion between fiber and nanoparticles. Bal and Behara (2006) suggest that an acid pretreatment with sulphuric acid for 48 h can break macromolecules, changing the microstructure of the polyester fiber. We believe the conditions polyester filter used in the present work (HCl at 0.01 M for 5 min) may affect the structure of the polyester, increasing the interaction and the adhesion between the fiber and the nanoparticle.

Biological analysis in the real environment

Figure 7 shows the results of the real environment in which the plates were ordered, as shown in Fig. 2.

The major difference between this analysis and another with a controlled colony of microorganisms (e.g., with *E. coli* or *S. aureus*) is that in a real environment it is impossible to control the growth of microorganisms and quantify it. Comparing the plates containing TSA as a culture medium and SAB (Fig. 7), it was observed that the fungi growth is more expressive in SAB. In the present work, fungi concentration in the environment was higher than the bacteria spores; however, the concentration depends on the season, hour of the day, temperature, humidity, and weather. Fungi have an aerodynamic diameter higher than 10 µm, while bacteria have an aerodynamic diameter between 3 and 5 µm (Qian et al. 2012), and the fungi spores can be captured by inertial impaction (Li et al. 2014). The higher the spore size, the higher the probability of the spore being captured by the fibers of the filter by inertial impaction in the filter structure (Li et al. 2014).

Comparing the growth of fungi, especially in Fig. 7 (II, d) and (III, f), it was observed the untreated filter (1st line of plates) showed more growth of microorganisms than the filter CuNP treated (third line of plates). The filamentous growth (hyphae) is characteristic of fungi, while bacteria are due to the colonial growth commonly in spherical growth. In general, it was observed a decrease in the growth of microorganisms when compared with the untreated filter and the CuNP-treated filter, indicating that the presence of those nanoparticles mitigates the presence of pathogens on the surface of the filter in air conditioning systems.

Even with a lower quantity of growth, the untreated HEPA (second of plates) and the HEPA of the CuNP-treated filter (fourth of the plates), we verify a reduction of the growth of microorganisms. To support this argument, other studies should be done, but in our opinion, the passage of the spores through the CuNP-treated filter can damage the microorganism spore, leading to a lower concentration of microorganisms in the air filtered.

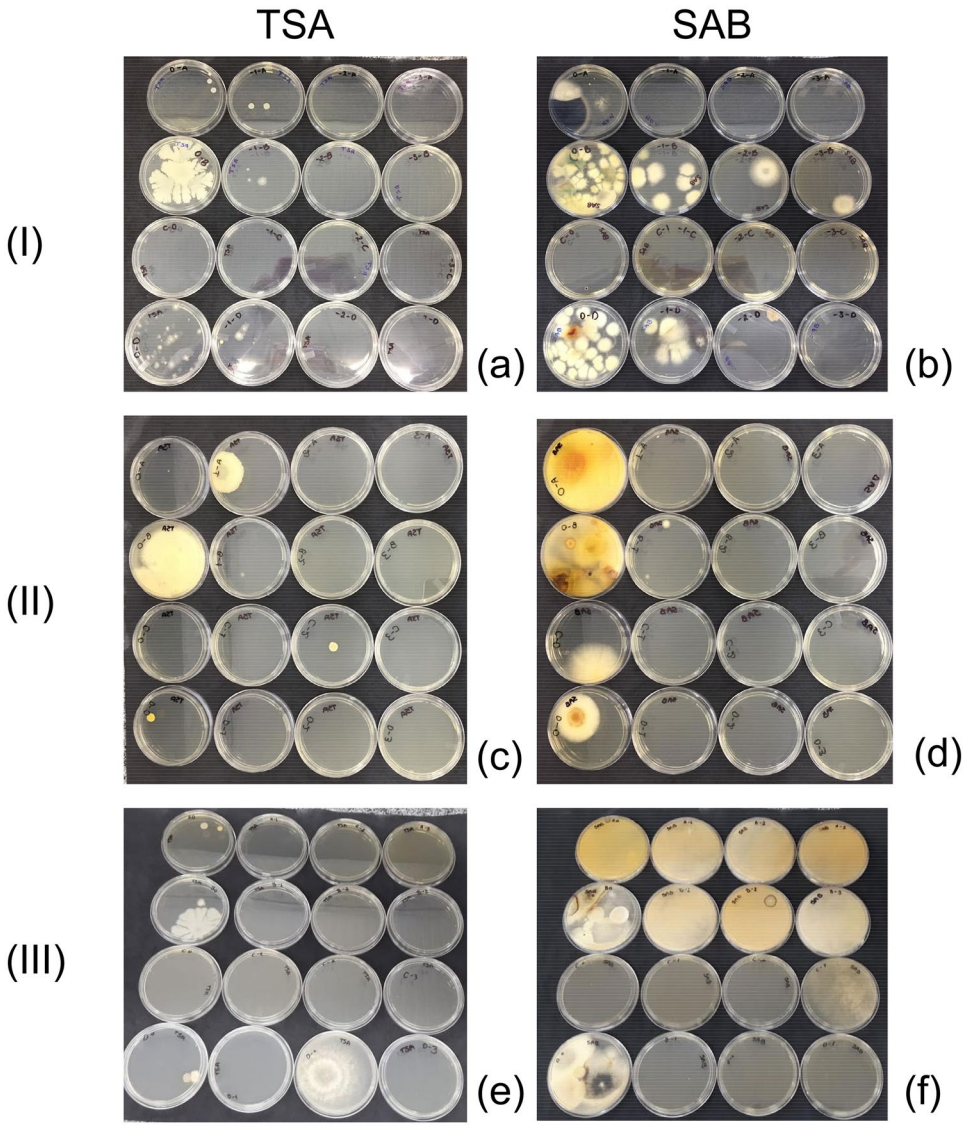

Fig. 7 Plates and the microorganism growth of three environments: **a** and **b** 1 h inside the Chemical Engineering Department bathroom; **c** and **d** in the Chemical Engineering Department hall for 6 h, and in an external environment for 24 h (**e** and **f**). TSA and SAB were the agar, where the microbial growth occurred

Conclusions

CuNPs [composed of metallic copper (Cu^0) and cuprous oxide (Cu_2O)] were synthesized by a redox reaction and applied in a commercial polyester filter for solid–gas filtration. The commercial polyester filter was submitted to an acid pretreatment previous CuNP coating and it was observed that the acid treatment increased the adhesion between fiber and nanoparticles. The presence of CuNP in the fiber filter nor the acid pretreatment previous CuNP coating interfered with permeability, which was in the order of 10^{-9} m^2. The modified filter was tested in loco and it was demonstrated that the CuNP in the fiber filter mitigates both fungi and bacterial growth. These results described that CuNPs applied in filters have a great promise as an antimicrobial agent in the development of smart systems for air filtration. Modified filters can be used in air conditioning systems or portable purifiers, enhancing the safety against microbes in indoor environments, where most transmissions happen.

Acknowledgements Authors thank the support of The National Council for Scientific and Technological Development (CNPq) Process No. 132697/2019-0 and Coordination of Improvement of Higher Education Personnel (CAPES), Grant/Award Number: CAPES-EPIDEMICS 88887.512003/2020-00.

Author contributions KM conducted the experiments, data analysis and wrote the manuscript. MLA and AB conceived the research ideas. CWOS contributed to the microbiological analysis. All the authors have discussed the results and approved the final version of the manuscript.

Data availability Not applicable.

Code availability Not applicable.

Declarations

Conflict of interest No known competing financial interests or personal relationships could have appeared to influence this paper.

References

Ahlawat A, Wiedensohler A, Mishra SK (2020) An overview on the role of relative humidity in airborne transmission of sars-cov-2 in indoor environments. Aerosol Air Qual Res 20:1856–1861. https://doi.org/10.4209/aaqr.2020.06.0302

Albanese A, Tang PS, Chan WCW (2012) The effect of nanoparticle size, shape, and surface chemistry on biological systems. Annu Rev Biomed Eng 14:1–16. https://doi.org/10.1146/annurev-bioeng-071811-150124

Anban EJ, Vel S (2015) Development of needle-punched nonwoven fabrics from reclaimed fibers for air filtration applications. Int J ChemTech Res. https://doi.org/10.1177/155892501400900117

AshaRani PV, Mun GLK, Hande MP, Valiyaveettil S (2009) Cytotoxicity and genotoxicity of silver nanoparticles in human cells. ACS Nano 3:279–290. https://doi.org/10.1021/nn800596w

Bal S, Behera R (2006) Structural investigation of chemical treated polyester fibers using saxs and other techniques. J Miner Mater Charact and Eng 5(2):179–198. https://doi.org/10.4236/jmmce.2006.52013

Balcilar M, Ozdemir ZA (2019) The volatility effect on precious metals price returns in a stochastic volatility in mean model with time-varying parameters. Phys A 534:122329. https://doi.org/10.1016/j.physa.2019.122329

Baley C, Busnel F, Grohens Y, Sire O (2006) Influence of chemical treatments on surface properties and adhesion of flax fibre-polyester resin. Compos A Appl Sci Manuf 37:1626–1637. https://doi.org/10.1016/j.compositesa.2005.10.014

Bogdanovic U, Lazi V, Vodnik V et al (2014) Copper nanoparticles with high antimicrobial activity. Mater Lett 128:75–78. https://doi.org/10.1016/j.matlet.2014.04.106

Bortolassi ACC, Guerra VG, Aguiar ML (2017) Characterization and evaluate the efficiency of different filter media in removing nanoparticles. Sep Purif Technol 175:79–86. https://doi.org/10.1016/J.SEPPUR.2016.11.010

Bortolassi ACC, Nagarajan S, de Araújo LB et al (2019) Efficient nanoparticles removal and bactericidal action of electrospun nanofibers membranes for air filtration. Mater Sci Eng C 102:718–729. https://doi.org/10.1016/j.msec.2019.04.094

Cammarano A, De Luca G, Amendola E (2013) Surface modification and adhesion improvement of polyester films. Cent Eur J Chem 11:35–45. https://doi.org/10.2478/s11532-012-0135-x

Catranis CM, Anagnost SE, Zhang L et al (2006) A new sub-sampling method for analysis of air samples collected with the Andersen single-stage sampler. Aerobiologia 22:177–184. https://doi.org/10.1007/s10453-006-9030-2

de Rosa PF, Aguiar ML, Bernardo A (2017) Modification of cotton fabrics with silver nanoparticles for use in conditioner air to minimize the bioaerosol concentration in indoor environments. Water Air Soil Pollut. https://doi.org/10.1007/s11270-017-3429-y

Garciá De Abajo FJ, Hernández RJ, Kaminer I et al (2020) Back to normal: an old physics route to reduce SARS-CoV-2 transmission in indoor spaces. ACS Nano 14:7704–7713. https://doi.org/10.1021/acsnano.0c04596

Hashimoto K, Sunada K, Miyauchi M et al (2017) Method for inactivating a virus. Sci Rep. https://doi.org/10.1038/s41598-022-09402-7

Hashmi M, Ullah S, Kim IS (2019) Copper oxide (CuO) loaded polyacrylonitrile (PAN) nanofiber membranes for antimicrobial breath mask applications. Curr Res Biotechnol 1:1–10. https://doi.org/10.1016/J.CRBIOT.2019.07.001

Holder CF, Schaak RE (2019) Tutorial on powder X-ray diffraction for characterizing nanoscale materials. ACS Nano 13:7359–7365. https://doi.org/10.1021/acsnano.9b05157

Hu X, Zhou Q (2013) Health and ecosystem risks of graphene. Chem Rev 113:3815–3835

Hwang GB, Heo KJ, Yun JH et al (2015) Antimicrobial air filters using natural *Euscaphis japonica* nanoparticles. PLoS ONE 10:1–15. https://doi.org/10.1371/journal.pone.0126481

Jeyaraj JM, Arumugam M, Kulandaiappan V (2015) A study on the functional proprieties of silk and polyester/lyocell mixed fabric. Revista Matéria 20:924–935. https://doi.org/10.1590/S1517-707620150004.0097

Li P, Wang C, Zhang Y, Wei F (2014) Air filtration in the free molecular flow regime: a review of high-efficiency particulate air filters based on Carbon Nanotubes. Small 10:4543–4561

Liu QM, Yasunami T, Kuruda K, Okido M (2012) Preparation of Cu nanoparticles with ascorbic acid by aqueous solution reduction method. Transact Nonferrous Metals Soc China 22:2198–2203. https://doi.org/10.1016/S1003-6326(11)61449-0

Machry K, de Souza CWO et al (2021) Prevention of pathogen microorganisms at indoor air ventilation system using synthesized copper nanoparticles. Can J Chem Eng. https://doi.org/10.1002/cjce.24272

Miguel AF (2003) Effect of air humidity on the evolution of permeability and performance of a fibrous filter during loading with hygroscopic and non-hygroscopic particles. J Aerosol Sci 34:783–799. https://doi.org/10.1016/S0021-8502(03)00027-2

Nakamura S, Sato M, Sato Y et al (2019) Synthesis and application of silver nanoparticles (Ag nps) for the prevention of infection in healthcare workers. Int J Mol Sci. https://doi.org/10.3390/ijms20153620

Nguyen VT, Trinh KS (2019) In situ deposition of copper nanoparticles on polyethylene terephthalate filters and antibacterial testing against escherichia coli and Salmonella enterica. Braz J Chem Eng 36(4):1553–1560. https://doi.org/10.1590/0104-6632.20190364s20190208. Accessed 16 Aug 2022

Patil V, Singh R, Kanade K, Yi G-R (2022) Copper nanomaterials derived preventive technologies for COVID-19 pandemic: a review. Adv J Chem Sect A 5:1–9. https://doi.org/10.22034/AJCA.2022.296509.1275

Qian J, Hospodsky D, Yamamoto N et al (2012) Size-resolved emission rates of airborne bacteria and fungi in an occupied classroom. Indoor Air 22:339–351. https://doi.org/10.1111/j.1600-0668.2012.00769.x

Ramírez-García G, Trapiella-Alfonso L, D'Orlyé F, D'Orlyé A (2018) Electrophoretic methods for characterizing nanoparticles and evaluating their bio-interactions for their further use as diagnostic, imaging, or therapeutic tools. Capill Electromigr Sep Methods. https://doi.org/10.1016/B978-0-12-809375-7.00019-8

Tang L, Zhu L, Tang F et al (2018) Mild synthesis of copper nanoparticles with enhanced oxidative stability and their application in antibacterial films. Langmuir 34:14570–14576. https://doi.org/10.1021/acs.langmuir.8b02470

Tremiliosi GC, Simoes LGP, Minozzi DT et al (2020) Ag nanoparticles-based antimicrobial polycotton fabrics to prevent the transmission and spread of SARS-CoV-2. bioRxiv. https://doi.org/10.1101/2020.06.26.152520

Warnes SL, Little ZR, Keevil CW (2015) Human coronavirus 229E remains infectious on common touch surface materials. Mbio. https://doi.org/10.1128/mBio.01697-15

Yao M, Zhang L, Ma J, Zhou L (2020) On airborne transmission and control of SARS-Cov-2. Sci Total Environ 731:139178. https://doi.org/10.1016/j.scitotenv.2020.139178

Zhu M, Han J, Wang F et al (2017) Electrospun nanofibers membranes for effective air filtration. Macromol Mater Eng. https://doi.org/10.1002/mame.201600353